

## Synthesis and Characterization of Novel Zeolite-X For Small Molecule Adsorption.

Shittu A.<sup>1</sup>, Okeniyi. S. O<sup>2</sup>, Omale P.<sup>2</sup>

1. Department of Science Education, School of Technical Education, Yaba College of Technology Yaba Lagos, Nigeria.

2. Department of Chemistry, Nigerian Defence Academy Kaduna State, Nigeria

[abdulrazakshittu@gmail.com](mailto:abdulrazakshittu@gmail.com)

### Abstract

Zeolite Na-X was successfully synthesized from Oke-Ako raw kaolin clay. The clay was soaked in water, beneficiated, and calcined at 650°C for three hours to obtain a more reactive amorphous metakaolin. The metakaolin was dealuminated using 60wt% tetraoxosulphate (VI) acid and washed to neutrality using a gravimetric method after reactions for five, ten, and fifteen minutes, respectively. The gel formed was aged for five days at room temperature and subjected to crystallization at a temperature of 110°C for reaction times of 8 hrs. The samples of raw, beneficiated, metakaolin and the synthesized zeolite-X were characterized using XRF, XRD, SEM, FT-IR and (Brunauer-Emmett-Teller (BET) analytical techniques. The XRF analysis confirmed the status of the raw kaolin and gave a positive status of the pretreatment and zeolitization processes. The intensity of crystallinity value from XRD were recorded for beneficiated, metakaolin and zeolite-X at 8hrs crystallization reaction time, while the SEM of the synthesized zeolite-X at 8hrs tends to be more desirable. Determination of the chemical and elemental compositions by X-ray Fluorescence (XRF), crystalline phases by X-ray Diffraction (XRD), surface morphology by Scanning Electron Microscopy (SEM) and molecular vibration of units by Fourier Transform Infrared Spectrophotometry (FT-IR) were done. The results showed that the zeolite-X synthesized from the Oke-Ako kaolin (OAK) was more crystalline/larger with sharper peaks on both XRD and FTIR. The XRF of Si/Al values of 1.95 and 1.78 were obtained for D5ZNa-X and ZNa-X respectively from Oke-Ako kaolin samples. XRD results supported the XRF values. Sharper zeolitic characteristic O-H stretching bands at 3362 cm<sup>-1</sup> was recorded and Si-O Stretching band at 969 Cm<sup>-1</sup> for both samples. The specific surface area of 266.97 m<sup>2</sup>/g was observed in ZNa-X sample with larger surface area than D5ZNa-X of specific surface area of 105.747m<sup>2</sup>/g. The results confirmed that zeolites-X was produced from Oke-Ako kaolin samples when compared with other results from literature. Generally the performance evaluation could be summarized that, these results illustrate the intricate interplay of different parameters on ammonia adsorption capacity using zeolites, providing valuable insights into the behaviour of zeolite as adsorbents in ammonia removal processes for optimizing ammonia removal applications and developing efficient, sustainable environmental remediation solution.

**Keywords:** Beneficiation, Metakaolin, Dealumination, X-Ray Fluorescence, (Brunauer-Emmett-Teller (BET), Crystallization, Zeolitization.

Sample Codes - (OAK) Oke-Ako Kaolin.;  
- (ZNa-X) Calcinated Zeolite-X.  
- (D5ZNa-X) Dealuminated five min. Zeolite-X.

## **Introduction**

Zeolites are an important class of crystalline, micro porous, aluminosilicate materials with a three dimensional fully cross linked open framework structures that form uniformly sized pores of molecular dimensions. (Adefila and Olakunle, 2008).

Zeolite have various industrial applications as adsorbents in separations, ion exchange ability, purification processes, environmental pollution control, molecular sieve and acidic catalysts for size and shape selective catalytic reactions. ((Perez, *et al.*, 2022, Ren, *et al.*, 2014, Maldonado, *et al.*, 2013). There are many types of natural zeolites that have been identified; they are in various forms such as clinoptilolite, mordenite, stilbite, phillipsite, chabazite, and limonite, (Vera-puerto *et al.*, 2020). Zeolites are stable solid and can resist high temperatures since they have melting points over 1000°C. The use of cheap and readily available materials such as kaolin to serve as a combined source of silica and alumina is highly desirable. The use of Oke-Ako Nigerian kaolin (OANK) to prepare zeolite-X is for an improved industrial value development. Nowadays, commercial synthetic zeolites are used more frequently than natural zeolites due to their purity of the crystalline products and the uniform particle sizes (He *et al.*, 2021, Cavallaro *et al.*, 2004). The main advantages of synthetic zeolites in comparison to natural ones are that they can be engineered with extensive variety of pore sizes and chemical properties and thermally stability. (Noviello *et al.*, 2021, Song *et al.*, 2004). In spite of the wide usage of Kaolin for the synthesis of Zeolites no attempt has been made previously to develop Zeolite from Oke-Ako Ijebu-Ode kaolin clay under various operating conditions. In this research work, full characterization of Nigerian Kaolin clay from Oke-Ako Ijebu-Ode deposit was processed.

## **Materials and Method**

### **Sample collection**

The starting material tagged (ROA) was geo-referenced from Oke-Ako village in Ijebu–Ode local government area of Ogun State, Nigeria.

### **Beneficiation of Sample**

Exactly 1.5 kg of the Oke-Ako kaolin was soaked with water for a duration of six days, in order to purify it from physically and chemically presence impurities such as soluble salts, grits and metallic oxides of Fe<sub>2</sub>O<sub>3</sub>, MgO, Na<sub>2</sub>O CaO, CaCO<sub>3</sub>, etc. to Finally the solid cake was split into smaller sizes and open dried in the laboratory for 4 days and further dried at 150°C in an electric oven for 4 hours, after which it was milled and subsequently packaged in a plastic sample container with cover for analysis and calcination. (Ayele, 2018)

### **Calcination of Sample.**

In this process, the Beneficiated sample was heated in a programmed Muffle electric furnace from room temperature (T) (31°C) to the calcinations temperature T<sub>cal</sub> of (650°C) for 3hrs. by evenly placing 500 grams of beneficiated kaolin evenly on a Ceramic crucible to allow for a relative good heat distribution, in order to improve the specific heat capacity and latent heat of kaolin. The metakaolin obtained was then cooled in a desiccator, prior to characterization and usage. (Macivers *et al.*, 2020)

## Dealumination of Calcined Clay

The prepared metakaolin was then treated using H<sub>2</sub>SO<sub>4</sub> in order to get the desired Si/Al values of 1.9 to 2.5 by reducing the alumina contents in the metakaolin. This is because each type of synthetic zeolite depends on the Si/Al value for its synthesis. The dealumination reaction was carried out at a temperature range of between 90-100°C using the conventional method and at ambient temperature for alternative method using 60% molar H<sub>2</sub>SO<sub>4</sub>.

**Equation 3.1:**  $\text{Al}_2\text{O}_3 (\text{s}) + 3\text{H}_2\text{SO}_4 (\text{aq}) \leftrightarrow \text{Al}_2 (\text{SO}_4)_3 (\text{aq}) + 3\text{H}_2\text{O} \dots$  Dealumination.

In this study, the conventional dealumination and the alternative method were used in the dealumination of the metakaolin. The method involved the reaction of the metakaolin with Sulphuric acid (H<sub>2</sub>SO<sub>4</sub>) and deionized water, with the application of heat from the heating mantle for conventional method and direct reaction of the sulphuric acid with the metakaolin sample at ambient temperature. Samples were added for reaction to commence and proceed for a specified reaction time of 5, 10, 15 minutes for both methods respectively. As soon as the reaction time elapsed, the reaction was terminated by adding enough distilled water. The resulting mixture were separated using gravimetric method. Dealuminated metakaolin obtained was continuously washed with distilled water until the absence of sulphate ion was confirmed (Bawa *et al* 2017)

## Gel Formation

The Silica/Alumina (SiO<sub>2</sub>/Al<sub>2</sub>O<sub>3</sub>) values used in this work is obtained from the compositional analysis of the dealuminated samples as shown in Table 4.3, The volume of water and the mass of sodium hydroxide required for gelating 30g of dealuminated metakaolin was at a molar concentration dilution of 2.8M for, 26g of Sodium hydroxide pellets in a teflon bottle and mixed with the required quantity of deionized water until the sodium hydroxide pellets were dissolved completely after been thoroughly mixed using a magnetic stirrer, 30g of dealuminated metakaolin sample was then added to the NaOH solution. The content was continuously stirred with magnetic stirrer to achieve homogeneity for 10 minutes. The resulting aluminosilicate

gel was put in an autoclave reactor, sealed and left in a static condition to age for 4 days at ambient conditions and crystallized for 8 hrs. (Olaremu *et al.*, 2018) The reaction mixtures was washed and filtered with deionized water until the pH of the filtrate is neutral to pH meter, finally the samples were dried overnight at 100°C before material characterization. (Ayele *et al.*, 2018).

**Equation 3.2:**  $6\text{Al}_2\text{Si}_2\text{O}_7 (\text{metakaolinite}) + 12\text{NaOH} \rightarrow \text{Na}_{12} (\text{AlO}_2)_{12} (\text{SiO}_2)_{12} + 6\text{H}_2\text{O}$   
(zeolite-X gel formation).

## Gel Aging

Gel aging can be considered as, an interval composition reaction of the gel and the crystallization process. In this synthesis, the gel was kept undisturbed (aged) at ambient temperature. To study the effect of gel aging time the samples were prepared to age for (4days) and crystallized for 8 hours at 110 °C as the optimum crystallization condition for Zeolites synthesis (Ayele *et al.*, 2018)

## Crystallization

The enclosed gel found in the autoclave reactor was then placed in the electric oven at 110 °C for 8 hours for crystallization of Zeolite to take place, The reaction was then quenched with

cold water to cease the crystallization process. Olaremu *et al.*, (2018). The zeolite formed was washed thoroughly several times with deionized water, The pH was monitored, while washing, using Micro Processor pH- meter to obtain a pH of 8. The precipitated solid was filtered, air dried in the laboratory for 24hrs and finally dried in an oven at 100 °C for 4 hours. The crystals were then pulverized for characterization.

### Adsorption Experiments on Performance Test.

The batch adsorption experiment was generally carried out using an adsorbent loading of 20 mg, at pH of 4-9 and at a room temperature of 25°C. During the experiment, 15 mL of 2 mg/L concentration of NH<sub>3</sub> solution was added to 20 mg of zeolite-based materials in a cuvette, and the absorbance was collected over a period of 2 hours. This procedure was repeated using 4, 8, and 12 hours interval study the effect of time on equilibrium (Al-Sheikh *et al.*, 2020).

From the adsorption experiments, the adsorption capacity,  $qt$  (mg/g) equation (1), which represents the amount of dye adsorbed per unit weight of zeolite and the NH<sub>3</sub> removal efficiency, ( $R\%$ ) equation (2), were calculated as follows:

$$\text{Adsorption capacity, } qt = \frac{(C_0 - C_t)V}{W}$$

$$\text{Removal efficiency (\%), } R = \frac{C_0 - C_t}{C_0} \times 100$$

Where  $C_0$  is the ammonia concentration at time  $t = 0$  (mg/L),  $C_t$  is the ammonia concentration at time  $t = t$  (mg/L),  $V$  is the volume of ammonia solution (mL), and  $W$  is the mass of adsorbent used (mg). The absorbance was measured using UV-Vis spectrophotometer at the ammonia characteristic monochromatic wavelength ( $\lambda$  max) of 340 nm.

## Results and Discussion

### Results of X-ray Fluorescence (XRF)

The results on Table 4.1 show that raw Oke-Ako kaolin contains contaminations of oxides of iron, titanium and Calcium, with increased value of these oxides listed, with the value of SiO<sub>2</sub> increased from 44.05% to 56.57% due to compensation of the whole proportion. The Table also show that Oke-Ako kaolin is ferric in nature due to its high content of iron oxide as compared with that of calcium oxide. It can also be observed that there is removal of Na<sub>2</sub>O following the purification processes. Pure raw kaolin clay has a Silica/Alumina value of between 1.5 to 3.5. (Ayele *et al.*, 2015, Ajayi *et al.*, 2010, Fentaw, 1998). The table 4.1 shows that the SiO<sub>2</sub>/Al<sub>2</sub>O<sub>3</sub> value of 3.21 and 2.97 for the raw and beneficiated kaolin respectively are within theoretical value (Villemiana *et al.*, 2019) There was also a gradual decrease in the moisture content from the raw sample to the metakaolin sample, also an increased in the value of the loss in ignition (LOI) from raw sample to beneficiated sample which eventually dropped in metakaolin value sample.

### XRF Analysis

The XRF data showed the expected high Si: Al value range of 1.90 to 1.95 for the alternative and 15.52 to 18.60 for the conventional methods respectively for zeolite-X synthesis from Oke-Ako samples stated in table 4.2. However, the results showed that a better ratio was achieved for both calcined sodium zeolite-X (ZNa-X) and dealuminated 5min sodium zeolite-X (D5ZNa-X) after treatments, compared to the raw Oke-Ako kaolin.

The result of X-ray diffraction (XRD) pattern for the raw Oke-Ako kaolin (OAK) analysis of the peaks show many sharp peaks, with low intensity at  $2\theta = 12.34^\circ$ . This is the main peak used in the identification of kaolinite clay (Ramirez, 2007). Also, the peak obtained at position corresponding to  $2\theta = 27.90^\circ$  indicated the presence of large quantities of quartz. Kaolinite and quartz are predominant characteristics of natural kaolin (Tracy and Higgins, 2007, Ayele, L *et al.*, 2015). Hence, the high level of quartz in Oke-Ako kaolin is not surprising because it is in agreement and similar to Ayele *et al.*, (2015). The noticeable difference is in the values of the Loss on ignition (LOI) which increased from 7.66% to 8.83% for raw and beneficiated samples while there was a decrease in the metakaolin sample to 1.16% respectively this was due to the burning off of impurities such as Illite, orthoclase, osumilite e. t. c during calcination. As evident in Table 4.1, the compositional analysis of the beneficiated Oke-Ako kaolin indicates an increased in the composition of its free silica, alumina, titanium and other impurities using the conventional method of purification. It is expected that purification or beneficiation of raw Oke-Ako kaolin had shifted down its silica/alumina ( $\text{SiO}_2/\text{Al}_2\text{O}_3$ ) value from 3.2 to 2.9. While the value of sodium oxide recorded 00. 0 due to complete removal during beneficiation.

### **Metakaolinization of Oke-Ako kaolin.**

The XRF analysis of metakaolin presented in Table 4.1 shows that there were reduction in the oxides of  $\text{Fe}_2\text{O}_3$ ,  $\text{TiO}_2$  from 4.68 to 2.28 and 4.42 to 2.24 respectively in chemical composition of the calcined Oke-Ako kaolin due to organic components and impurities burnt out. The noticeable difference is in the values of  $\text{Na}_2\text{O}$  which decreased from 27.79 to 0. 00 with a slight reduction in the  $\text{SiO}_2 / \text{Al}_2\text{O}_3$  ratio from 2.97 to 1.78 for beneficiated and calcined samples respectively. As a result, the calcination of Oke-Ako kaolin from room temperature to  $450^\circ\text{C}$  brings a loss in one of the sharp peaks as observed in Figure 4.6 due to the loss of the hydration water, which results in a better ordering in the structure of the kaolin molecules. However, there was complete loss of the main peaks reflection at  $650^\circ\text{C}$  leaving only a small holes which indicate the formation of a non- crystalline phase. This is in good agreement with results of (Martinez *et al* 2013), which show the formation of metakaolin at a temperature around  $650^\circ\text{C}$ . The peaks at  $2\theta = 12.34^\circ$  (kaolinite peak) disappeared but the peak at  $2\theta = 26.67^\circ$  was not affected by the thermal treatment, attributed to the presence of quartz. Therefore, metakaolin can be described as an amorphous material containing free silica, free alumina as reported by (Edomwonyi-Otu *et al.*, 2013). The compositional silica /alumina ratio was reduced to 1.78 after calcination.

### **Dealumination of Metakaolin Sample.**

Dealumination is an alternative route to reduce the alumina content from the metakaolin, as a results it increases the  $\text{SiO}_2: \text{Al}_2\text{O}_3$  values of the starting material. Adjusting the silica to alumina ratio was the key steps in the starting gel of high silica zeolite-X synthesis. Increased in the composition of its free silica, alumina, titanium and other impurities using the conventional method of dealumination, which was not similar to alternative method due to slight decrease in some of the parameters below. (Babalola *et al* 2015).

### **X-Ray Diffraction Analysis of D5ZNa-X and ZNa-X Zeolite-X.**

Powder X-ray diffraction was used to determine the sample crystallinity. The formation of zeolite-X from Oke-Ako kaolin was ascertained by comparing its XRD pattern of record to that of International Zeolite Association (IZA) powder pattern identification diffractograms, indicating a Faujasite structure (FAU). As illustrated by Treacy and Higgins within a range of  $2\theta = 5-50^\circ$ , the first peak for zeolite X will appear within  $6-10^\circ$ . (Treacy *et al.*, 2001). The first three strongest peak for each zeolite (D5ZNa-X) was observed at  $2\theta=6.76^\circ$ ,  $12.95^\circ$  and  $24.95^\circ$

then  $2\theta = 6.33^\circ$ ,  $26.8^\circ$  and  $31.2^\circ$ , for ZNa-X as both Zeolites have similar gel aging time of four day respectively. Small zigzag peaks refer to the presence of amorphous material. Strong peaks represent full crystallization. Also the SEM graphs represented by Plates 4.1a and 4.1b respectively have also confirmed the successful synthesis of zeolite-X. Synthesized zeolite-X gave similar FT-IR spectrum and SEM morphology patterns. (Kovo *et al.*, 2012) and (Ekpe *et al.*, 2017).

Figure 4.1 is showing the superimposed of the two synthesized Zeolites D5ZNa-X and ZNa-X, subtend at the  $2\theta$  (Theta) Bragg's angles  $6.33^\circ$ ,  $26.80^\circ$ ,  $31.20^\circ$  for ZNa-X and the Bragg's angles for D5ZNa-X were  $6.76^\circ$ ,  $12.95^\circ$  and  $24.95^\circ$  respectively. However, the Quartz subtends at the  $2\theta$  (Theta) Bragg's angles of  $20.10^\circ$ ,  $27.20^\circ$ ,  $60.90^\circ$  for ZNa-X and the quartz for D5ZNa-X subtends at the  $2\theta$  (Theta) Bragg's angles of  $20.10$ ,  $27.00^\circ$  and  $68.01^\circ$  respectively. Therefore, showed sharp peaks, indicating that both samples were crystalline at this stage. The patterns matched with both synthetic and commercial Na-X zeolite XRD patterns as reported by (Bai *et al.*, 2018). It was also similar to the (not de-aluminated) untreated metakaolin reported by (Konne *et al.*, 2016). The sharper peaks and lower broad background on the XRD pattern of Oke-Ako indicated that the D5ZNa-X was more crystalline while the untreated calcined ZNa-X has a larger surface area value, which were the main characteristics of zeolite-X.

Table 4. 1 XRF Compositional analysis results of the Raw, Beneficiated and Calcined Oke-Ako Kaolinite.

Oke-Ako Kaolinite (Wt. %)			
OXIDES	Raw Oke-Ako Kaolinite.(Wt %)	Beneficiated Oke Ako Kaolinite.(Wt%)	Calcined Oke-Ako Kaolinite.(Wt%)
SiO <sub>2</sub>	44.05	56.57	43.26
Al <sub>2</sub> O <sub>3</sub>	23.33	32.34	41.39
Fe <sub>2</sub> O <sub>3</sub>	1.77	4.68	2.28
TiO <sub>2</sub>	2.04	4.42	2.24
Na <sub>2</sub> O	27.79	0.00	0.00
CaO	0.04	0.12	0.08
Total	99.02	98.13	89.25
Moisture content	1.38	0.14	0.05
L.O.I*	7.66	8.83	1.16
SiO <sub>2</sub> /AlO <sub>3</sub> ratio	3.21	2.97	1.78

Loss on ignition\*

Table 4.2X-ray fluorescence (XRF) compositional analysis of Dealuminated Oke-Ako Metakaolin using Novel and Conventional method with various dealumination time.

De-Alumination		Novel Method			Conventional Method		
Oxide	Metakaolin	5 minutes	10 minutes	15 minutes	5 minutes	10 minutes	15 minutes
SiO <sub>2</sub>	43.26	43.61	43.11	45.59	46.82	84.06	85.94
Al <sub>2</sub> O <sub>3</sub>	41.39	38.02	38.53	40.58	40.96	9.21	7.85
Fe <sub>2</sub> O <sub>3</sub>	2.28	2.12	2.04	2.19	0.67	1.24	1.05
TiO <sub>2</sub>	2.24	2.23	2.14	2.28	1.99	3.60	3.37
Na <sub>2</sub> O	---	--	--	---	18.96	0.00	0.00
CaO	0.07	0.03	0.04	0.03	0.23	0.34	0.12
SiO <sub>2</sub> /Al <sub>2</sub> O <sub>3</sub>	1.78	1.95	1.90	1.90	1.95	15.52	18.60

**Table 4.3** Revealed the XRD results of the BOK, COK, D5ZNa-X and ZNa-X.

Sample	Kaolinite Peak positions	Quartz Peak positions
BOA	<a href="#">12.34°</a> (14%)( <a href="#">Ramirez, 2007</a> ).	27.90° (55%) <a href="#">Ayele, L. et al., 2015</a>
COA	Nil	26.67° ( <a href="#">Edomwonyi-Otu, et al., 2013</a> ).
D5 ZNa-X	2θ = 6.76°, 12.95° and 24.95°	20.10°, 27.00° and 68.01°
ZNa-X	2θ = 6.33°, 26.8° and 31.2°, ( <a href="#">Kovo et al 2010</a> ) and <a href="#">Ekpe et al 2017</a> ).	27.50°, 60.2°, and 60.9°

Table 4.4 Revealed the FT-IR summary Data cm<sup>-1</sup> range of all the Samples

Assignments	BOK	COK	D5ZNa-X	ZNa-X	Literature	Reference
OH Stretch Vibration	3690	—	—	—	3694	<a href="#">Rios.A et al (2008)</a>
OH absorbed H <sub>2</sub> O molecule	—	—	3362	3362	3447	<a href="#">Weia.G et al (2015)</a>
H <sub>2</sub> O adsorption Band	—	—	1651	1640	1645	<a href="#">Pandianga.K et al (2017)</a>
C=C bond in aromatic comps	—	—	1394	—	1430	<a href="#">Taju.S (2016)</a>
Si-O-Si Stretching	988	—	969	969	1005	<a href="#">Elizabeth.V (2016)</a>
Symmetric Si-O-Si Stretching	790	790	—	—	797	<a href="#">Aniela.Z (2017)</a>
Asymmetric Si-O- Si Stretching	1114	1058	—	—	1035	<a href="#">Aniela.Z (2017)</a>

Table 4.5 Revealed the BET Analysis results of D5ZNa-x and ZNa-X

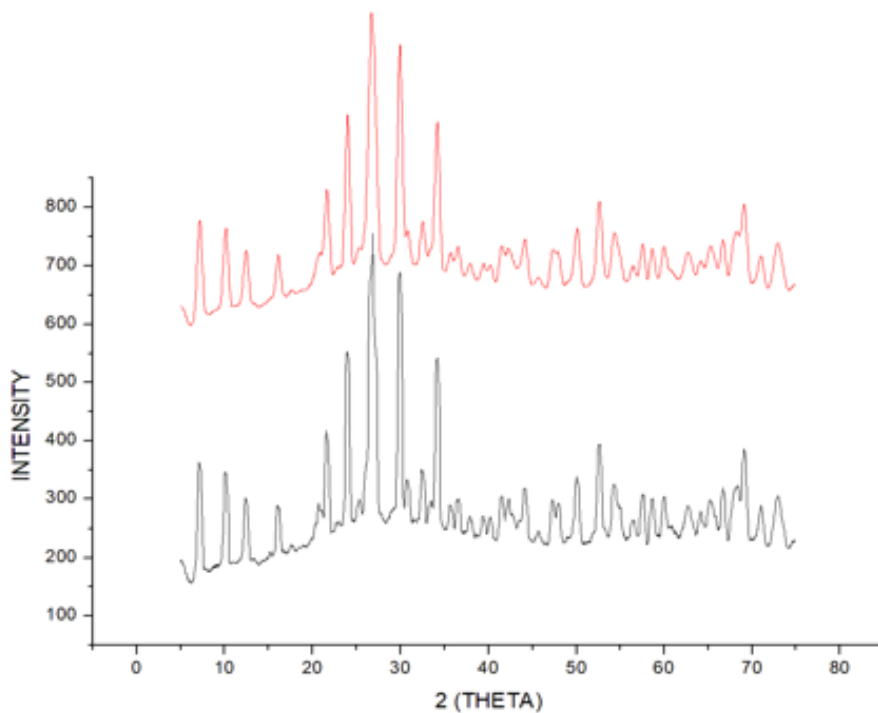
SAMPLE	BET SURFACE AREA(m <sup>2</sup> /g)	PORE VOLUME (cc/g)
ZNa-X	323.62	0.165
D5ZNa-X	145.85	0.131

Table 4.6a Revealed the summary of percentage minerals in D5ZNa-X sample.

Mineralogy of D5ZNa-X	Percentage
Zeolites	30.5%
Quartz	51.6%
Nitrolite	0.8%
Mordenite	0.7%

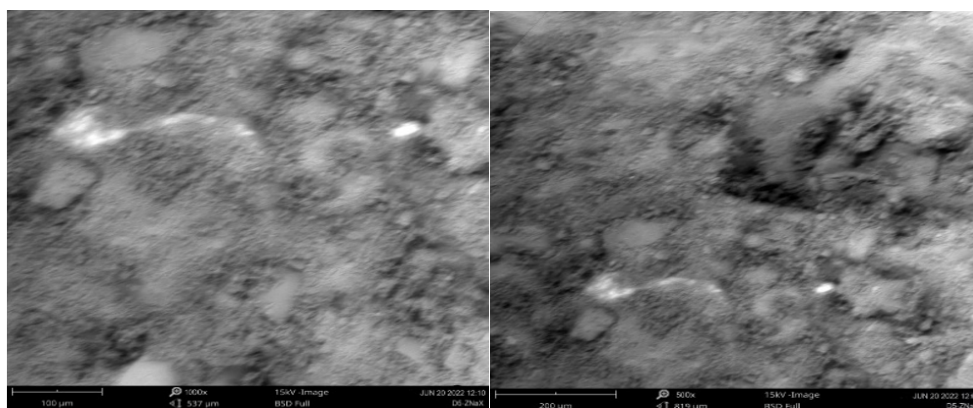
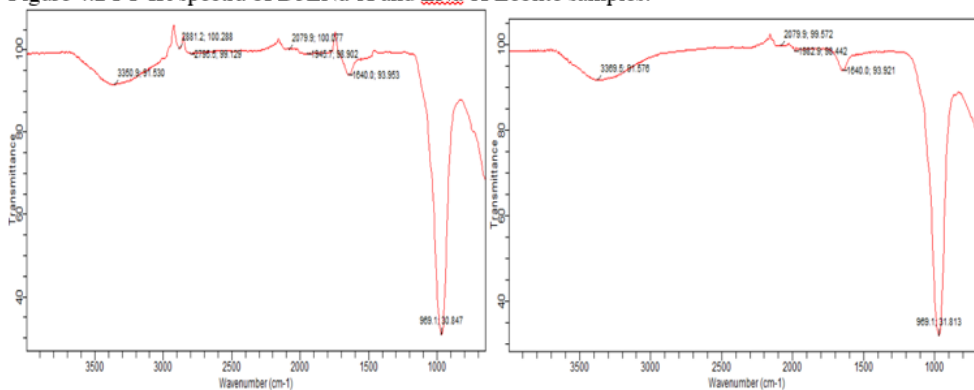
Table 4.6b Revealed the percentage mineral content of ZNa-X sample.

Mineralogy of ZNa-X sample	Percentage (%)
Zeolites	25%
Quartz	50%
Mordenite	0.8%
Nitrolite	0.5%



**Figure 4.1** Showing the XRD pattern of superimposed ZNa-X and D5ZNa-X.

**Figure 4.2** FT-IR spectra of D5ZNa-X and ZNa-X Zeolite samples.



**(4.1.a)** SEM image of D5ZNa-X sample

**(4.1.b)** SEM image of ZNa-X sample

**Plate 4.1a** SEM Image of D5ZNa-X at x100 $\mu$ m. **Plate 4.1b** SEM Image of ZNa-X at x100 $\mu$ m.



## FT-IR (Fourier Transformed Infra-Red)

### FT-IR Analysis.

Fourier Transformed Infra-Red analysis was carried out on BOA, COA, D5ZNa-X and ZNa-X. The characterization was carried out between 650 and 4000  $\text{cm}^{-1}$ . Strong bands at 3690, 3652, 3452  $\text{cm}^{-1}$  were observed for the beneficiated sample. No prominent peak was observed between 3000 and 1100  $\text{cm}^{-1}$  except in 2083 for calcined sample. A number of peaks with variable intensities were observed in the range of 1200  $\text{cm}^{-1}$  – 800  $\text{cm}^{-1}$  region for the beneficiated sample.

However, the transmittance intensity was reduced in the calcined sample (from 10% to 45%) and the peaks even out in the COA, in the same vein the calcination resulted in loss of OH peaks which were present in the beneficiated sample at 3690  $\text{cm}^{-1}$ . This could be associated with increased in porosity due to metakaolinization. Therefore, strong peaks (low transmittance) at 3450  $\text{cm}^{-1}$  (OH region) indicates the zeolites has an abundance of hydroxyl group (Adeyanju *et al.*, 2016, Lu *et al.*, 2019). in ZNa-X and D5ZNa-X respectively. The higher intensity of the D5ZNa-X peaks above the ZNa-X agreed with the XRD and SEM of higher crystallinity of D5ZNa-X over ZNa-X. (Pandianga, K *et al.*, 2017).

FT-IR spectroscopy in Table 4.4 was used to probe the structures of D5ZNa-x and ZNa-X and to monitor reactions in zeolite pores. The FT-IR spectrum bands at 3690  $\text{Cm}^{-1}$  Beneficiated Oke Ako kaolin (BOA) correspond to the OH stretching vibrations on the surface of kaolinite (Rios. A. *et al.*, 2008). A critical examination of the results revealed some major changes in the spectra of the samples.

These are:

1. A shift in the wave number of adsorption from a lower wave number to a higher wave number was observed (hyperchromic effect). In this case, the intensity of the adsorption band was found to increase in D5ZNa-X (Ameh *et al.*, 2015).
2. Disappearance and appearance of some adsorption band of the samples for BOA and COA is as a result of calcination on ZNa-X while D5ZNa-X is as a result of dealumination. The extent of the frequency shift can be directly attributed with the high level of specific molecular interactions such as hydrogen and dipole-dipole interactions. From the results obtained, hypochromic shifts were observed for C-N stretch and C=C stretch. Those functional groups, missing might have been used for the formation of new bands (El-Yukub *et al.*, 2020).

### Analysis of Brunauer-Emmett-Teller (BET).

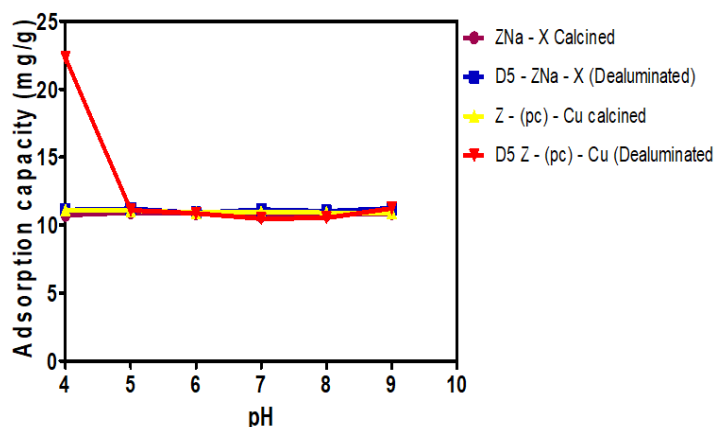
The Table 4.5 above shows BET results of calcined and dealuminated samples of Zeolites. D5ZNa-X had a lower specific surface area value of 145.85  $\text{m}^2/\text{g}$  and pore volume of 0.090  $\text{cc}/\text{g}$ . The surface area of D5ZNa-X decreased by 151% on dealumination for 5 minutes while the pore volume decreased exponentially by 30%. The decreased in the surface area may be attributed to dealumination process of the kaolin mineral to the highly amorphous metakaolin as shown by the XRD patterns of the materials. The ordered platelets structure of kaolinite as a result of calcination as shown by SEM images had resulted into highly surface area in ZNa-X than the dealuminated D5ZNa-X sample (Bansiwal *et al.*, 2010).

## Impact of pH on the percentage removal of ammonia using four different prepared zeolite-based adsorbents

The impact of pH values on NH<sub>3</sub> adsorption by using the prepared zeolites adsorbents were performed by adjusting pH values in a range from 4.0 to 9.0. Figure 4.13 depicts the adsorption capacities of the four different zeolite-based adsorbent. The results indicate a clear pH-dependent behavior in ammonia adsorption capacity using ZNa – X (Calcined neat Zeolite sample).

At pH 4, the adsorption capacity was found to be 10.73 mg/g. The highest adsorption capacity of 10.90 mg/g was achieved at pH 5. However, beyond pH 5, a slight decrease in adsorption capacity was observed. The adsorption capacity at pH 6 was found to be 10.84 mg/g. The adsorption capacity generally increased as the pH level shifted from acidic (pH 4) to neutral (pH 7). This trend can be attributed to the increasing presence of uncharged ammonia (NH<sub>3</sub>) molecules at lower pH, which can readily interact with zeolite surfaces. However, the adsorption capacity increases at pH levels of 8 and 9 with the values of 10.74 and 10.85 mg/g respectively. This may be due to the abundance of hydroxide ions (OH<sup>-</sup>) in the solution which may compete with ammonia for adsorption sites, leading to a reduction in adsorption capacity (Lina *et al.*, 2013). At lower pH values (acidic conditions), ammonia exists predominantly as uncharged NH<sub>3</sub> molecules, which are more easily adsorbed.

For D5 – ZNa–X (Dealuminated neat Zeolite sample), the results proved that the adsorption process in the current study was somewhat pH-dependent. The adsorption capacity of ammonia was highest at pH 9 with a value of 11.23 mg/g while the lowest was found at pH 6 with a value of 10.89 mg/g. The present study observed the same trend in a pH rise with other literatures (Safie *et al.*, 2019).

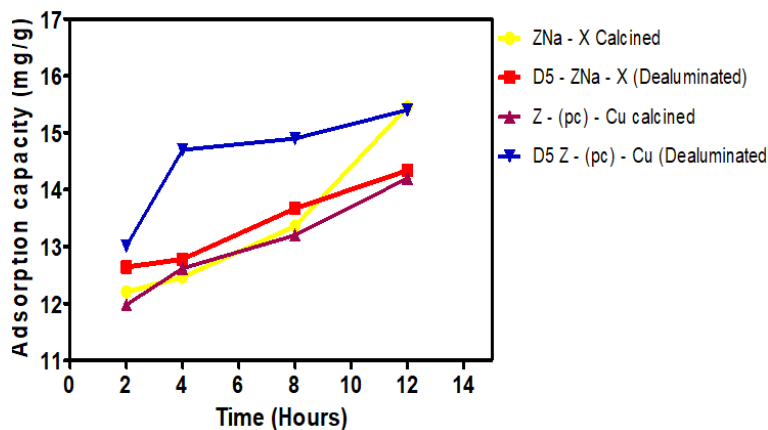


## Impact of pH on NH<sub>3</sub> adsorption capacity by four different adsorbent.

### Impact of time on the percentage removal of ammonia using four different prepared zeolite-based adsorbents.

At the 2-hour mark, the adsorption capacity is 12.21 mg/g. This represents the initial rapid adsorption phase, where ZNa - X Calcined quickly capture ammonia from the solution due to available adsorption sites. As time progresses to 4 hours, the adsorption capacity increases to 12.46 mg/g. This indicates that ammonia adsorption onto adsorbents continues to occur, albeit at a slightly reduced rate compared to the initial phase. By the 8-hour mark, the adsorption capacity reaches 13.36 mg/g. This suggests that ammonia adsorption is approaching equilibrium, where the rate of adsorption becomes nearly equal to the rate of desorption. At this point, further increases in adsorption capacity are minimal. Finally, at the 12-hour mark, the

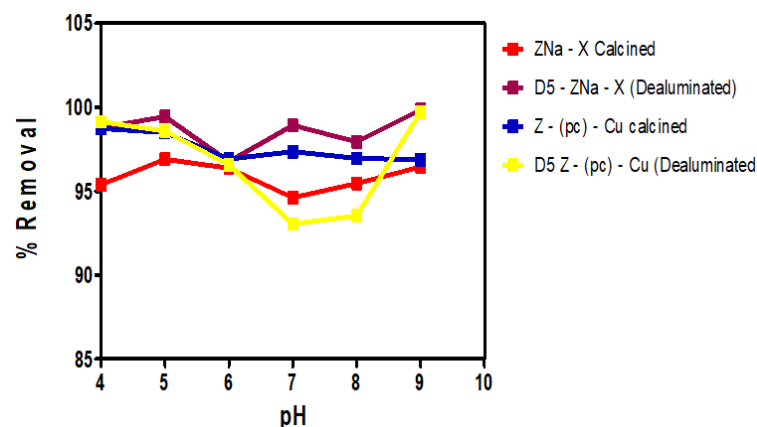
adsorption capacity stabilizes at 15.45 mg/g. This value represents the maximum ammonia adsorption capacity achievable under the given conditions and highlights that ZNa-X Calcined have effectively captured ammonia from the solution. Similar findings was observed for D5 - ZNa - X (Dealuminated); 12.64mg/g at 2-hour mark, 12.78mg/g at 4-hour mark, 13.67mg/g at 8-hour mark and 14.34mg/g at 12-hour mark, Z - (pc) - Cu calcined catalyst; 11.98mg/g at 2-hour mark, 12.62mg/g at 4-hour mark, 13.20mg/g at 8-hour mark and 14.20mg/g at 12-hour mark, and D5 Z - (pc) - Cu (Dealuminated; 13.01 mg/g at 2-hour mark, 14.70mg/g at 4-hour mark, 14.90 mg/g at 8-hour mark and 15.40 mg/g at 12-hour mark. The results are presented in Figure 4.14. Generally, the graphs show that the amount of NH<sub>3</sub> molecules adsorbed increased with contact time for all the adsorbents.



#### Impact of time on NH<sub>3</sub> adsorption capacity by four different adsorbent.

#### Effect of pH on the percentage removal of ammonia using four different prepared zeolite-based adsorbents.

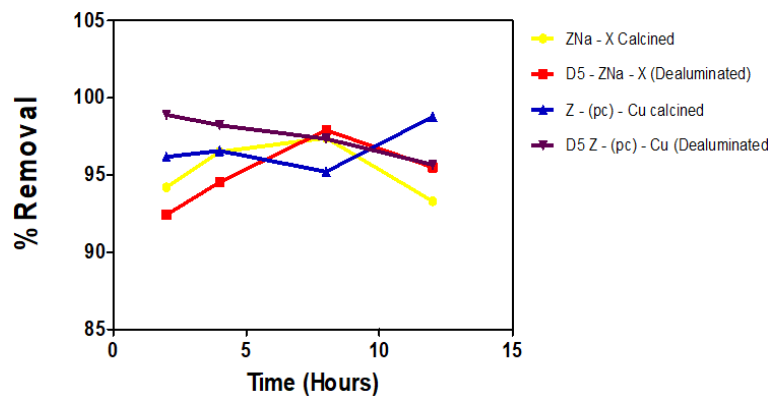
The impact of pH values on NH<sub>3</sub> adsorption by using the prepared adsorbents were performed by adjusting pH values in a range from 4.0 to 9.0. As shown in Figure 4.15, among the initial pH values, the maximum ammonia adsorption takes place at pH 5.0 with the value of 96.90%. The percentage removal increased as the pH level shifted from acidic (pH 4) to (pH 6). The values are found to be 95.39, 96.90 and 96.37% at pH 4, 5 and 6 respectively. This trend is consistent with the increased presence of ammonia (NH<sub>3</sub>) molecules at lower pH levels, which are more easily adsorbed by ZNa-X Calcined. The increase in ammonia removal at increased pH and initial ammonia concentration suggests the interplay of molecular adsorption mechanism (Weia *et al.*, 2015).



#### Impact of time on NH<sub>3</sub> removal efficiency from liquid by four different adsorbent.

**Impact of time on the percentage removal of ammonia using four different prepared zeolite-based adsorbents.**

At the 2-hour mark, the percentage removal of ammonia is 94.20%. During this early stage, a substantial portion of ammonia has been adsorbed by the ZNa - X Calcined, but the removal process is ongoing. As time progresses to 4 hours, the percentage removal increases to 96.50%. This indicates that the ammonia removal process continues to improve with time, with more ammonia molecules being captured by the zeolite adsorbents. By the 8-hour mark, the percentage removal reaches 97.40%. This suggests that the ammonia removal process is approached optimal efficiency, with a significant portion of ammonia removed from the solution (Nyankson et al., 2019). This value represents the maximum ammonia removal efficiency achievable under the given conditions (Sanchez-Hernandez et al., 2018). Finally, at the 12-hour mark, the percentage removal reduced to 93.30%.



**Impact of time on the removal of NH3 by the adsorbents.**

**Table 4.** Showing the removal of NH3 by ZNa-X Calcined sample.

$C_0$ (mg/L)	pH	%ABSORBANCE	$C_t$ (mg/L)	% Removal	Adsorption capacity (mg/g)
15	4	0.268	0.692	95.39	10.73
15	5	0.180	0.465	96.90	10.90
15	6	0.211	0.545	96.37	10.84
15	7	0.313	0.808	94.61	10.64
15	8	0.264	0.681	95.46	10.74
15	9	0.206	0.532	96.45	10.85

**Table 4.** —Showing the removal of NH<sub>3</sub> by D5ZNa-X Dealuminated sample

C <sub>o</sub> (mg/L)	pH	%ABSORBANCE	C <sub>t</sub> (mg/L)	%Removal= $\frac{C_o - C_t}{C_o} \times 100$	A. capacity, qt = $\frac{(C_o - C_t)V}{W}$
15	4	0.071	0.185	98.77	11.11
15	5	0.032	0.084	99.44	11.19
15	6	0.188	0.486	96.76	10.89
15	7	0.062	0.162	98.92	11.13
15	8	0.120	0.311	97.93	11.02
15	9	0.008	0.023	99.85	11.23

**Table 4.** —Showing the % removal of NH<sub>3</sub> by the samples.

Time (hours)	ZNa - X Calcined	D5 - ZNa - X (Dealuminated)
2.00	94.20	92.43
4.00	96.50	94.53
8.00	97.40	97.90
12.00	93.30	95.50

**Table 4.** —Showing the effect on adsorption capacity by the samples.

Time (hours)	ZNa - X Calcined	D5 - ZNa - X (Dealuminated)
2.00	12.21	12.64
4.00	12.46	12.78
8.00	13.36	13.67
12.00	15.45	14.34

## Conclusion

This chapter present the conclusion and recommendations based on the obtained results, the following conclusions can be drawn. Zeolite-X was successfully synthesized from clay sourced from Oke-Ako of Ijebu-Ode, Ogun state, Nigeria after alkaline treatment of its metakaolin. This work demonstrated the development of hydrothermal process to produce an important industrial catalyst (zeolite-X) from locally sourced Kaolin. The X-ray fluorescence (XRF), X-ray diffraction (XRD) analysis confirmed the presence of zeolitic mineral phases in both D5ZNa-X and ZNa-X crystallized samples respectively.

However, the D5ZNa-X sample was more crystalline as shown by sharper intense XRD peaks, rougher surface on the SEM micrograph and sharper bands on the FT-IR. Both samples had similar bands especially the characteristic zeolitic O-H stretching at 3362Cm<sup>-1</sup> and Si-O Stretching at 969 cm<sup>-1</sup>.

The XRF showed the presence of higher silica to alumina ratios of 1.95 and 1.78 after treatments and also showed the absence of some toxic metals implying that the synthesized zeolites were safe and environmentally friendly. The zeolites formed have shown that the hydrothermal modification of reactive kaolin into zeolite-X depended solely on the ageing time, reaction temperature, metakaolinization temperature and NaOH concentration.

According to this study's results, the dealumination process was optional since, zeolite-X was synthesized successfully with or without the dealumination process, except in their percentage of crystallinity, as D5ZNa-X is more crystalline than ZNa-X

These results illustrate the intricate interplay of different parameters on ammonia adsorption capacity using zeolites. Dose-dependent, pH-dependent and concentration-dependent trends were observed, providing valuable insights into the behaviour of zeolite adsorbents in ammonia removal processes. Understanding these trends is fundamental for optimizing ammonia removal applications and developing efficient, sustainable environmental remediation solution.

### **Recommendation**

A lot of work has been done in this area and has successfully produced high quality synthesized zeolites like zeolite A, X and Y from Nigerian kaolin. However, zeolite-X synthesis from novel Oke-Ako will have a greater role as a catalyst in adsorption of small molecules. Using natural raw material like Kaolin will cut down cost considerably as local materials are cheaper than purchasing chemicals

### **References**

- Adefila, S., Ajayi, A. and Atta, Y. (2007) Synthesis of Faujasite Zeolites from Kanakara Kaolin Clay. *Journal of Applied Sciences Research*, 3, 1017-1021.
- Adeyanju, O., Olademehin, O. P., Nwanta, U. C., Adejoh, A. I., Hussaini, Y., & Plavec, J. (2016). Synthesis and characterization of carboxymethyl *Plectranthus esculentus* starch. A potential disintegrant. *Journal of Pharmaceutical and Applied Chemistry*, 2 (3), 44-50.
- Ameh P. O Kohapu and Eddy N. O (2015). Experimental and quantum chemical studies on the corrosion inhibition potential of phthalic acid for mild steel in 0.1M H<sub>2</sub>SO<sub>4</sub> *chemical Sciences Journal* 6: 3.
- Aniela Z. (2017). Chemical modifications of hollow silica microspheres for the removal of organic pollutants in simulated wastewater. [Dissertation] Abdullah University of science and technology, Saudi Arabia; 201-207. anthelmintic carriers. *J Helminthol*.2000; pp.74: 137– 141.
- Al-Sheikh, F., Moralejo, C., Pritzker, M., Anderson, W. A., & Elkamel, A. (2020). Ammonia removal from real wastewater using a LEWATIT S 108 H resin: A batch process and fixedbed column. *Separation Science and Technolog*
- Ayele, L. (2018). Synthesis of zeolite A using raw kaolin from Ethiopia and its application in removal of Cr (III) from tannery wastewater. *Journal of Chemical Technology & Biotechnology*.93 (1): 146-154.
- Ayele, L., *et al*, (2016). Conventional versus alkali fusion synthesis of zeolite A from low grade kaolin. *Applied Clay Science*.132-133: 485-490.
- Babalola, R., *et al*, (2015). Comparative Analysis of Zeolite Y from Nigerian Clay and Standard Grade.
- Bai, H. -X., Zhou, L. -M., Chang, Z. -B., Zhang, C. and Chu, M. (2018) Synthesis of Na- X Zeolite from Longkou Oil Shale Ash by Alkaline Fusion Hydrothermal Method.

- Carbon Resources Conversion, 1, 245-250. <https://doi.org/10.1016/j.crcon.2018.08.005>
- Bansiwal A, Pillewan P, Biniwale R. B and Rayalu A. S (2010) Copper incorporated mesoporous Alumina for defluoridation of drinking water, microporous and mesoporous, 129: 54-61
- Cavallaro G, Pierro P, Palumbo FS, Testa F, Pasqua L, Aiello R. (2004). Drug delivery devices based on mesoporous silicate. *Drug Deliv.* 11, 41–46.
- Edomwonyi-otu, L. C., Aderemi, B. O., Ahmed, A. S., Coville, N. J., & Maaza, M. (2013). Influence of Thermal Treatment on Kankara Kaolinite. *Optican* 1826, 15 (5), 1–5. <http://doi.org/http://dx.doi.org/10.5334/opt.bc>
- Elizabeth V. (2016). Synthesis and characterization of zeolites from bauxite and kaolin: application to the removal of heavy metals from mining wastewater. [Dissertation] Kabwe: Kwame Nkrumah University, Zambia;
- El-Yaqub and S. O Okeniyi (2020) Corrosion studies of Aluminium alloy in 0.1M H<sub>2</sub>SO<sub>4</sub> by extracts of *balanitesaegyptiaca* Science view Journal (SCVJ) volume 1no 2 81-87.
- Ekpe, I., (2017). Zeolite Synthesis, Characterization and Application Areas: A Review. Vol.6.
- Emmanuel Nyankson, Jonas Adjasoo, Johnson Kwame Efavi, Reuben Amedalor, Abu Yaya, Gloria
- Pokuaa Manu, Kingsford Asare, and Nii Amarkai Amartey (2019). Characterization and Evaluation of Zeolite A/Fe<sub>3</sub>O<sub>4</sub> Nanocomposite as a Potential Adsorbent for Removal of Organic Molecules from Wastewater. *Hindawi Journal of Chemistry* Volume, Article ID 8090756, 13 pages <https://doi.org/10.1155/2019/8090756>
- He, Y., Tang, S., Yin, S., & Li, S. (2021). Research progress on green synthesis of various high-purity zeolites from natural material-kaolin. *Journal of Cleaner Production*, 306, 127248.
- Kovo, A. S. (2012). Effect of Temperature on The Synthesis of Zeolite X from Ahoko Nigerian Kaolin Using Novel Metakaolinitization Technique. *Journal of Chemical Engineering Communications*, Volume 199, - Issue 6 786-797. <http://dx.doi.org/10.1080/00986445.2011.625065>.
- Maciver, V. P., Dagde, K. K., & Konne, J. L. (2020). Synthesis of zeolite X from locally sourced kaolin clay from Kono-Boue and Chokocho, Rivers state, Nigeria. *Advances in Chemical Engineering and Science*, 10 (4), 399-407.
- Noviello, M., Gattullo, C. E., Faccia, M., Paradiso, V. M., & Gambacorta, G. (2021). Application of natural and synthetic zeolites in the oenological field. *Food Research International*, 150, 110737.
- Olaremu, A., Odebunmi, E. and Nwosu, F. (2018) Synthesis of Zeolite from Kaolin Clay from Erusu South western Nigeria. *Journal of Chemistry Society of Nigeria*, 43, 381-786.
- Ren, B, Bai, S. Y, Sun, J. H., Zhang, F. and Fan, M. (2014). “Controllable synthesis of obvious core-shell structured Y/Beta composite zeolite by a step wise induced method,” *RSC Advances*, vol.4, no.43, 22755–22758.

- Rios A, Williams D, Roberts L. (2008). Removal of heavy metals from acid mine drainage using coal fly ash, natural clinker and synthetic zeolites.: 156 (1-3): 23–35, 20: <https://doi.org/10.1016/j.jhazmat.2007.11.123>
- Ruth Sa'nchez-Herna'ndez, 1 Isabel Padilla, 1 Sol Lo'pez-Andre's, 2 and Aurora Lo'pez-Delgado (2018). Al-Waste-Based Zeolite Adsorbent Used for the Removal of Ammonium from Aqueous Solutions. Hindawi. International Journal of Chemical Engineering Volume 2018, Article ID 1256197, 11 pages <https://doi.org/10.1155/2018/1256197>.
- Song W, Justice RE, Jones CA, Grassian VH, Larsen SC. (2004) Synthesis, characterization, and adsorption properties of nanocrystalline ZSM- 5. *Langmuir*.20: 8301.
- Taju S. (2016). Synthesis of nano hydroxyapatite/ stilbite composite for defluoridation of drinking water. [dissertation] Addis Ababa University, Ethiopia.
- Treacy, M. M. J., & Higgins, J. B. (2001). Collection of simulated XRD powder patterns for zeolites. (5th ed.). Elsevier B. V. [http://doi.org/10.1016/S0166-9834\(00\)81382-2](http://doi.org/10.1016/S0166-9834(00)81382-2).
- Pandiangan K, Arief S, Jamarun N, Simanjuntak W. *J Mater Environ Sci* (2017). Synthesis of Zeolite-X from Rice Husk silica and aluminum metal as a catalyst for transesterification of palm oil.8 (5): 1797–1802.
- Pérez-Botella, E., Valencia, S., & Rey, F. (2022). Zeolites in adsorption processes: State of the art and future prospects. *Chemical Reviews*, 122 (24), 17647-17695.
- Vera-Puerto, I., Saravia, M., Olave, J., Arias, C., Alarcon, E., & Valdes, H. (2020). Potential application of chilean natural zeolite as a support medium in treatment wetlands for removing ammonium and phosphate from wastewater. *Water*, 12 (4), 1156.
- Weia G, Yanga L, Zhonga W, Li S. (2015). Fast removal of methylene blue from aqueous solution by adsorption onto poorly crystalline hydroxyapatite nanoparticles. *J NanomaterBiostruct*;10 (4): 1343–1363.